

# Isolated fourfold fermion in BiTeI

A. Kuibarov<sup>1</sup>, A. Fedorov<sup>1,5</sup>, V. Bezguba<sup>1,2</sup>, H. Berger<sup>3</sup>, A. Yaresko<sup>4</sup>,  
V. Voroshnin<sup>5</sup>, A. Kordyuk<sup>2</sup>, P. Baumgärtel<sup>5</sup>, B. Büchner<sup>1,6</sup> and S. Borisenko<sup>1</sup>

<sup>1</sup>*IFW Dresden, Helmholtzstrasse 20, 01069 Dresden, Germany*

<sup>2</sup>*Kyiv Academic University, 03142, Kyiv, Ukraine*

<sup>3</sup>*Institute of Condensed Matter Physics, Ecole Polytechnique Fédérale de Lausanne, Lausanne, Switzerland*

<sup>4</sup>*Max Planck Institute for Solid State Research, 70569, Stuttgart, Germany*

<sup>5</sup>*Helmholtz-Zentrum Berlin für Materialien und Energie, BESSY II, 12489 Berlin, Germany*

<sup>6</sup>*Institute for Solid State and Materials Physics, TU Dresden, 01062, Dresden, Germany*

November 6, 2024

## Abstract

We use angle-resolved photoemission spectroscopy to revisit the electronic structure of BiTeI, previously identified as a polar semiconductor with giant bulk Rashba splitting. We propose an alternative description which is based on the experimentally determined crystal structure and agrees well with resistivity, quantum oscillations and optical measurements. BiTeI emerges as a topological 3D Dirac semimetal hosting only two, well isolated from each other and rest of the band structure, Dirac points. Properly doped bulk material or the controlled synthesis of iodine-terminated surface of the pristine material promise to become a canonical condensed matter system whose physical properties are completely defined by the behaviour of fourfold fermions.

## 1 Introduction

A large number of topologically non-trivial band structures continue to be discovered theoretically and experimentally, perhaps weakly. Almost all of them have very limited practical use, mainly because of two fundamental problems: the presence of other, trivial electronic states at the Fermi level and the distance of the topological features from this level. While the former requires sophisticated, so far unrealistic, band engineering, the latter seems to be relatively easily overcome by doping the system with additional charge carriers. However, even shifting the Fermi level in e.g. "minimal" topological semimetals Cd<sub>3</sub>As<sub>2</sub> [1] and TaIrTe<sub>4</sub> [2] with only a few Dirac or Weyl points to match their energy location is quite challenging and remains unsuccessful. Therefore, it is important to find a system where the topological features are isolated from the trivial ones and their energy position can be easily manipulated.

BiTeI is one of the stable materials where the charge carriers concentration can be varied by doping of different atoms and which came to the focus of the research after a strong Rashba-like spin splitting of the bulk bands has been observed experimentally by ARPES [3]. Large spin-orbit splitting in the bulk is a requisite for a number of magnetotransport and optical effects including magnetic field generation by spin current [4], generation of spin current itself [5] or even non-centrosymmetric superconductivity [6]. Since then BiTeI has been intensely studied by various techniques including optical spectroscopy [7, 8, 9, 10], ARPES [3, 11, 12, 13, 14] and quantum oscillations [15, 16, 8]. Ambipolar conduction [12], enhanced infrared magneto-optical response [17], orbital textures [14] as well as signatures of pressure-induced quantum phase transition [18, 10, 19] have been found in this material during the next couple of years, accompanied by the theoretical studies [20, 21, 22, 23].

In spite of this attention, the fermiology of BiTeI remains controversial. Photoemission study using higher photon energies [11] found that the Rashba-like crossing parabolic dispersions seen in Ref. [3] and earlier interpreted as originating from the bulk are actually the surface states and that the true bulk states can be visible only using the higher photon energies. In contrast, Bowden et al. [14] observes two sets of Rashba-like dispersions persisting in a broad photon energy range and interprets them as originating from the quantum well states. The controversy as regards the origin of the Rashba-like states

and corresponding Fermi surface extends to quantum oscillation experiments. While C-R wang et al. and Bell et al. [15, 16] find the agreement with the theoretical three-dimensional Fermi surface, although never detecting the frequency corresponding to the vertical section of the Fermi surface along c-axis, Martin et. al [8] states that the observed oscillations support essentially two-dimensional Fermi surface. Moreover, Martin et. al finds that the quantum oscillations originate from the bulk states, contrary to the conclusions of most of the ARPES studies.

Intriguingly, the controversy may have its roots in a tiny difference in distances between the tellurium and iodine atoms from bismuth. Despite earlier [24] and later confirmed [25] experimental results on the crystal structure, it was the "relaxed" theoretical crystal structure proposed in the initial work [3] that was widely accepted by the community. If the experimental Bi-Te and Bi-I distances are swapped, the band structure changes significantly and implies a small and essentially three-dimensional Fermi surface.

In present study, we show that the band structure implied by the experiment [24, 25] describes the observations by numerous techniques more consistently. BiTeI turns out to be a unique 3D Dirac semimetal with only two 3D Dirac points maximally separated in k-space. Remarkably, there are no other electronic states within this 0.4 eV wide "Dirac band".

## 2 Materials and methods

BiTeI single crystals used in experiments were grown by vapour transport method. Experiments were carried out at One Square and U125-2 NIM stations of the BESSY synchrotron and IFW Dresden laboratory with laser light. Samples were cleaved *in situ* with pressure better than  $2 \cdot 10^{-10}$  mbar. Experiments were performed using 20-80 eV horizontal polarized synchrotron and 6 eV laser light. As an electron analyzers we used Scienta R400 with angular resolution  $0.2^\circ$ , and Fermiologics FeSuMa 1.0 [26] with  $0.2^\circ$  angular resolution.

## 3 Results and discussion

In Fig. 1 we show the differences between the crystal structures, band structures and Fermi surfaces caused by an alternative theoretical description based on relaxed atomic positions suggested earlier [3]. By now generally accepted picture implies that contrary to the experimental data, the distance between the bismuth and iodine layers should be larger than the one between the bismuth and tellurium layers. This change opens the energy gap turning the material from a 3D Dirac semimetal to a semiconductor and significantly alters the shape and dimensionality of the Fermi surface. The latter becomes essentially three-dimensional and consists of two separated "beans". As is seen from comparison of the near- $E_F$  band structures highlighted by the red circles in Fig. 1 (d,e) this occurred because of different behavior and different number of the bands along the  $\Gamma$ A-direction.

Before we start presenting new ARPES data which will allow us to identify which version of the band structure from Fig. 1 corresponds to BiTeI, we mention that previous ARPES studies identified two terminations of the surface of BiTeI. These are not expected to be observed from the same cleave if the crystal is ideal, but with the presence of the stacking faults [12, 13] their presence can be understood. In any case, since the iodine-terminated surface appears to be hole-rich thus leaving the Rashba-like states unoccupied, less stable and is subjected to ageing [13], we carried out our experiments trying to pick up the signal from the Te-terminated parts.

In Fig. 2a we show a Fermi surface map taken using 25 eV photons. In this case the FS contours look conventional, consisting of two, mostly circular but with some hexagonal warping, features, as in the previous ARPES studies [3, 11, 12, 13, 14]. These FS contours alone are not sufficient to distinguish between two cases since both FS (Fig. 1a and Fig. 1c) have similar horizontal sections in high-symmetry points, A and  $\Gamma$ /A respectively. We note, that upon closer consideration, the map in Fig. 2a does contain remnants of the feature in between small and large FS and the smaller one looks broader, possibly because of small additional splitting. This is not expected in the case of theoretical 3D-Fermi surface (Fig. 1a). The only occupied flat portion of the band along  $\Gamma$ A-direction near A-point (Fig. 1d) implies only one set of Fermi surface contours in ARPES maps because of moderate  $k_z$ -resolution of the method, which implies an integration of the band structure over significant part of perpendicular momentum. In contrast, two flat portions of the bands along  $\Gamma$ A in the experimental band structure (Fig. 1e) fully agree with the presence of two sets of the FS contours in the integrated along  $k_z$ -spectrum. We also note a

light asymmetry of the underlying dispersion with respect to the zeroth momentum along  $k_y$ -direction shown in Fig. 1c. This is not surprising, since the trigonal warping is naturally present in a material with no inversion symmetry.

According to the calculations, the 3D FS from Fig. 1c should have more such  $180^\circ$  asymmetric sections than the one implied by the "relaxed" model. In Fig. 2b we present the FS map which corresponds perhaps to the maximum distortion of this kind. Recorded with 15 eV photons, this map does deviate from the one from Fig. 2a and, actually, from all ARPES data published earlier. Trigonal warped FS contours are supported by clearly asymmetric dispersion seen in Fig. 2d. This dataset rules out any artificial asymmetry of the FS maps, which may be caused by rotating the sample or scanning the signal electronically through the entrance slit of conventional hemispherical analyzer. The Fig. 2d represents an energy-momentum distribution taken along the entrance slit while keeping all other experimental parameters fixed. Such a modification of the 2D section of the FS clearly speaks in favour of bulk origin of the detected electronic states and cannot be explained neither by surface contribution or quantum well states.

In order to bring photon energies and  $k_z$ -scale in correspondence, we recorded the normal emission spectra as a function of  $h\nu$  (Fig. 3a). Comparing the data to the band structures from Fig. 1d,e one can unambiguously identify the band dispersing by approximately 0.7 eV from  $\Gamma$  to A immediately below the bands forming the 3D Dirac point. We note, that "relaxed" band structure implies *two* features in this region, not observed experimentally. Now we can estimate the inner potential ( $V_0 = 11$ ) in the free-electron approximation and identify photon energies corresponding to the high symmetry points along  $k_z$  using  $k_z = 0.512\sqrt{(E_k + V_0)}$ , where  $E_k$  is electron kinetic energy.

With this information we can now sample the 3D Fermi surface in that portion of BZ along  $k_z$  which will allow us to distinguish between two scenarios. We also switch to another way of detecting the photoelectrons, namely to the technology [26] that allows the Fermi surface map to be detected at once without rotating the sample or scanning the electron beam. This approach minimizes the influence of the matrix elements by keeping the geometry of the experiment constant and enables isotropic momentum resolution. In Fig. 3b,c we compare the calculated FS section going through the  $\Gamma$ -point with the FS map taken at 22 eV. Apart from the slight differences in size, the agreement is remarkable - the sharp and clearly resolved features with symmetric and hexagonal shapes are fully reproduced. This is in sharp contrast to the "relaxed" calculations (Fig. 1a), which predict no FS at  $\Gamma$  and therefore only blurred contributions from other  $k_z$ s are expected in ARPES due to the moderate resolution along this direction. The model based on experimental crystal structure also implies that going away from  $\Gamma$ -point towards A-point the FS section should become strongly trigonally warped. Also this observation is clearly supported by the ARPES data. In Fig. 3d,e we show the corresponding results, which again are in a full qualitative agreement. We emphasize that using the new technology the intensity distribution is minimally influenced by the experimental geometry, free from stripes due to scanning, and thus reproduces spectral function more precisely.

We have also performed experiments using a 6-eV laser. According to the universal curve, the escape depth of the photoelectrons in this case is larger than in any previous ARPES study of BiTeI, and the spectra are therefore most representative of the bulk. In addition, the ultimate momentum resolution along  $k_x$  and  $k_y$  enables exact alignment of the sample and identification of all features. Such low photon energy also means that  $k_z$ -resolution becomes worse and the radius of the sphere in k-space probed by ARPES is minimal. Both factors lead to integration of the signal along  $k_z$ . Nevertheless, the result presented in Fig. 4 exactly corresponds to our scenario and contradicts the "relaxed" model as well as interpretations in terms of the surface states - both sets of parabolic features suggested by Fig. 1e are present and thus are of bulk origin. Remarkably, these two sets of Rashba-like split parabolas are observed now in a very broad photon energy range, where the resolution is sufficient to detect them: from 6 eV here via 22-70 eV interval in Ref. [14] up to 93 eV in e.g. Ref. [12] (Fig. S3). There was no evidence for the breaks implied by essentially 3D FS (Fig. 1a) in this photon energy range.

Finally, we try to locate the 3D-Dirac points implied by our description of BiTeI directly. The Figure 5a shows a Dirac point in momentum-energy cut taken using 64 eV photons. It is seen at approximately 0.48 eV binding energy as a typical crossing of two dispersing features. As expected for such binding energies, this crossing appears blurred due to the increased scattering. Tuning the photon energy away from this  $k_z$  towards the  $\Gamma$ -point, we observe no evidence for the crossing at 74 eV photon energies in Figure 5b in a full agreement with the 3D electronic structure implied by Fig. 1e. We also present an attempt to find more Dirac points in momentum space considering in Fig. 5c a map of intensity in  $(k_z, k_y)$  plane

corresponding to the determined above energy of Dirac crossing (0.48 eV). Band structure in Fig. 1e implies pairs of 3D Dirac points centered at A-points when going along  $k_z$  since the crossing is closer to A- than to  $\Gamma$ -point. In qualitative agreement with this expectation we do observe the localization of intensity near A-points. However, experiment shows that shift of Dirac points towards A-point is even larger since two Dirac points are not seen split near A-points resulting in the elongated along  $k_z$  intensity maxima.

Our ARPES results prove that BiTeI is not a semiconductor as previously thought, but rather a 3D Dirac semimetal with a unique isolation of two Dirac points from the rest of the band structure features, both in terms of energy and momentum. Its quasi-two-dimensional Fermi surface (Fig. 1c) is in an excellent agreement with resistivity measurements [3] and all quantum oscillation studies [8, 15, 16], which never detected a frequency corresponding to the orbits in  $(k_z, k_x / k_y)$ -planes. As our calculations of the optical response show Fig. 6, it is hard to distinguish between two scenarios when Fermi level is shifted by  $\sim 300$  meV, as in the experiment. This makes all previous arguments in favour of agreement between the optics and ARPES valid also for our scenario for the pristine samples. However, the sharpness of the edge in optical conductivity for BiTeI with lower carriers concentration, as e.g. in Fig. 2 of Ref.[7], show better agreement with the calculations corresponding to the experimental crystal structure 6.

Having an ideal 3D Dirac semimetal with isolated Dirac points at the Fermi level would help to single out the physical properties caused exactly by fourfold fermions. It is hard to overestimate the value of such information since up to now only numerous theoretical studies predicted exotic physics and it was not possible to bring isolated 3D Dirac points to the Fermi level experimentally. A straightforward way would be to dope the system with holes, but usually such approaches are not successful. Our study of Te-terminated surface as well as previous ARPES and STM studies [27, 12, 13] of I-terminated surface imply that the latter is already very close to that ideal 3D-Dirac semimetal state. If the typical size of natural iodine termination is of the order of 100 nm size, it may become possible to stabilize and increase this area, so that devices can be built enabling a broad spectrum of experiments highlighting BiTeI from its new, different side.

## References

- [1] Sergey Borisenko, Quinn Gibson, Danil Evtushinsky, Volodymyr Zabolotnyy, Bernd Büchner, and Robert J. Cava. Experimental realization of a three-dimensional dirac semimetal. *Phys. Rev. Lett.*, 113:027603, Jul 2014.
- [2] E. Haubold, K. Koepernik, D. Efremov, S. Khim, A. Fedorov, Y. Kushnirenko, J. van den Brink, S. Wurmehl, B. Büchner, T. K. Kim, M. Hoesch, K. Sumida, K. Taguchi, T. Yoshikawa, A. Kimura, T. Okuda, and S. V. Borisenko. Experimental realization of type-ii weyl state in noncentrosymmetric  $\text{TaIrTe}_4$ . *Phys. Rev. B*, 95:241108, Jun 2017.
- [3] K. Ishizaka, M. S. Bahramy, H. Murakawa, M. Sakano, and T. Shimojima. Giant rashba-type spin splitting in bulk bitei. *Nature Materials*, 10(7):521–526, Jul 2011.
- [4] Ioan Mihai Miron, Gilles Gaudin, Stéphane Auffret, Bernard Rodmacq, Alain Schuhl, Stefania Pizzini, Jan Vogel, and Pietro Gambardella. Current-driven spin torque induced by the rashba effect in a ferromagnetic metal layer. *Nature Materials*, 9(3):230–234, Mar 2010.
- [5] Zhonghao Liu, Setti Thirupathaiah, Alexander N. Yaresko, Satya Kushwaha, Quinn Gibson, Wei Xia, Yanfeng Guo, Dawei Shen, Robert J. Cava, and Sergey V. Borisenko. A giant bulk-type dresselhaus splitting with 3d chiral spin texture in irbise. *physica status solidi (RRL) – Rapid Research Letters*, 14(4):1900684, 2020.
- [6] E. Bauer, G. Hilscher, H. Michor, Ch. Paul, E. W. Scheidt, A. Griбанov, Yu. Seropegin, H. Noël, M. Sigrist, and P. Rogl. Heavy fermion superconductivity and magnetic order in noncentrosymmetric  $\text{CePt}_3\text{Si}$ . *Phys. Rev. Lett.*, 92:027003, Jan 2004.
- [7] J. S. Lee, G. A. H. Schober, M. S. Bahramy, H. Murakawa, Y. Onose, R. Arita, N. Nagaosa, and Y. Tokura. Optical response of relativistic electrons in the polar bitei semiconductor. *Phys. Rev. Lett.*, 107:117401, Sep 2011.
- [8] C. Martin, E. D. Mun, H. Berger, V. S. Zapf, and D. B. Tanner. Quantum oscillations and optical conductivity in rashba spin-splitting bitei. *Phys. Rev. B*, 87:041104, Jan 2013.

- [9] A. A. Makhnev, L. V. Nomerovannaya, T. V. Kuznetsova, O. E. Tereshchenko, and K. A. Kokh. Optical properties of bitei semiconductor with a strong rashba spin-orbit interaction. *Optics and Spectroscopy*, 117(5):764–768, Nov 2014.
- [10] M. K. Tran, J. Levallois, P. Lerch, J. Teyssier, A. B. Kuzmenko, G. Autès, O. V. Yazyev, A. Ubaldini, E. Giannini, D. van der Marel, and A. Akrap. Infrared- and raman-spectroscopy measurements of a transition in the crystal structure and a closing of the energy gap of bitei under pressure. *Phys. Rev. Lett.*, 112:047402, Jan 2014.
- [11] Gabriel Landolt, Sergey V. Eremeev, Yury M. Koroteev, Bartosz Slomski, Stefan Muff, Titus Neupert, Masaki Kobayashi, Vladimir N. Strocov, Thorsten Schmitt, Ziya S. Aliev, Mahammad B. Babanly, Imamaddin R. Amiraslanov, Evgueni V. Chulkov, Jürg Osterwalder, and J. Hugo Dil. Disentanglement of surface and bulk rashba spin splittings in noncentrosymmetric bitei. *Phys. Rev. Lett.*, 109:116403, Sep 2012.
- [12] A. Crepaldi, L. Moreschini, G. Autès, C. Tournier-Colletta, S. Moser, N. Virk, H. Berger, Ph. Bugnon, Y. J. Chang, K. Kern, A. Bostwick, E. Rotenberg, O. V. Yazyev, and M. Grioni. Giant ambipolar rashba effect in the semiconductor bitei. *Phys. Rev. Lett.*, 109:096803, Aug 2012.
- [13] Sebastian Fiedler, Lydia El-Kareh, Sergey V Eremeev, Oleg E Tereshchenko, Christoph Seibel, Peter Lutz, Konstantin A Kokh, Evgueni V Chulkov, Tatyana V Kuznetsova, Vladimir I Grebennikov, Hendrik Bentmann, Matthias Bode, and Friedrich Reinert. Defect and structural imperfection effects on the electronic properties of BiTeI surfaces. *New Journal of Physics*, 16(7):075013, jul 2014.
- [14] Lewis Bawden, Jonathan M. Riley, Choong H. Kim, Raman Sankar, Eric J. Monkman, Daniel E. Shai, Haofei I. Wei, Edward B. Lochocki, Justin W. Wells, Worawat Meevasana, Timur K. Kim, Moritz Hoesch, Yoshiyuki Ohtsubo, Patrick Le Fèvre, Craig J. Fennie, Kyle M. Shen, Fangcheng Chou, and Phil D. C. King. Hierarchical spin-orbital polarization of a giant rashba system. *Science Advances*, 1(8):e1500495, 2015.
- [15] Chang-Ran Wang, Jen-Chuan Tung, Raman Sankar, Chia-Tso Hsieh, Yung-Yu Chien, Guang-Yu Guo, F. Chou, and Wei-Li Lee. Magnetotransport in copper-doped noncentrosymmetric bitei. *Physical Review B*, 88:081104(R), 08 2013.
- [16] C. Bell, M. S. Bahramy, H. Murakawa, J. G. Checkelsky, R. Arita, Y. Kaneko, Y. Onose, M. Tokunaga, Y. Kohama, N. Nagaosa, Y. Tokura, and H. Y. Hwang. Shubnikov–de haas oscillations in the bulk rashba semiconductor bitei. *Phys. Rev. B*, 87:081109, Feb 2013.
- [17] L. Demkó, G. A. H. Schober, V. Kocsis, M. S. Bahramy, H. Murakawa, J. S. Lee, I. Kézsmárki, R. Arita, N. Nagaosa, and Y. Tokura. Enhanced infrared magneto-optical response of the non-magnetic semiconductor bitei driven by bulk rashba splitting. *Phys. Rev. Lett.*, 109:167401, Oct 2012.
- [18] Xiaoxiang Xi, Chunli Ma, Zhenxian Liu, Zhiqiang Chen, Wei Ku, H. Berger, C. Martin, D. B. Tanner, and G. L. Carr. Signatures of a pressure-induced topological quantum phase transition in bitei. *Phys. Rev. Lett.*, 111:155701, Oct 2013.
- [19] Joonbum Park, Kyung-Hwan Jin, Y. J. Jo, E. S. Choi, W. Kang, E. Kampert, J.-S. Rhyee, Seung-Hoon Jhi, and Jun Sung Kim. Quantum oscillation signatures of pressure-induced topological phase transition in bitei. *Scientific Reports*, 5(1):15973, Nov 2015.
- [20] M. S. Bahramy, R. Arita, and N. Nagaosa. Origin of giant bulk rashba splitting: Application to bitei. *Phys. Rev. B*, 84:041202, Jul 2011.
- [21] G. A. H. Schober, H. Murakawa, M. S. Bahramy, R. Arita, Y. Kaneko, Y. Tokura, and N. Nagaosa. Mechanisms of enhanced orbital dia- and paramagnetism: Application to the rashba semiconductor bitei. *Phys. Rev. Lett.*, 108:247208, Jun 2012.
- [22] M. S. Bahramy, B.-J. Yang, R. Arita, and N. Nagaosa. Emergence of non-centrosymmetric topological insulating phase in bitei under pressure. *Nature Communications*, 3(1):679, Feb 2012.
- [23] Sebastian Schwalbe, René Wirnata, Ronald Starke, Giulio A. H. Schober, and Jens Kortus. Ab initio electronic structure and optical conductivity of bismuth tellurohalides. *Phys. Rev. B*, 94:205130, Nov 2016.

- [24] A V Shevelkov, E V Dikarev, R V Shapanchenko, and B A Popovkin. *J. Solid State Chem.*, 114:379, 1995.
- [25] Vladimir A. Kulbachinskii, Vladimir G. Kytin, Alexey A. Kudryashov, Alexei N. Kuznetsov, and Andrei V. Shevelkov. On the electronic structure and thermoelectric properties of bitebr and bitei single crystals and of bitei with the addition of bii3 and cui. *Journal of Solid State Chemistry*, 193:154–160, 2012. Solid State Chemistry and Materials Science of Thermoelectric Materials.
- [26] Sergey Borisenko, Alexander Fedorov, Andrii Kuibarov, Marco Bianchi, Volodymyr Bezguba, Paulina Majchrzak, Philip Hofmann, Peter Baumgärtel, Vladimir Voroshnin, Yevhen Kushnirenko, Jaime Sanches-Barriga, Andrey Varykhalov, Ruslan Ovsyannikov, Igor Morozov, Saicharan Aswartham, Oleg Feya, Luminita Harnagea, Sabine Wurmehl, Alexander Kordyuk, Alexander Yaresko, Helmuth Berger, and Bernd Büchner. Fermi surface tomography, 2021.
- [27] Christopher John Butler, Hung-Hsiang Yang, Jhen-Yong Hong, Shih-Hao Hsu, Raman Sankar, Chun-I Lu, Hsin-Yu Lu, Kui-Hon Ou Yang, Hung-Wei Shiu, Chia-Hao Chen, Chao-Cheng Kaun, Guo-Jiun Shu, Fang-Cheng Chou, and Minn-Tsong Lin. Mapping polarization induced surface band bending on the rashba semiconductor bitei. *Nature Communications*, 5(1):4066, Jun 2014.

## List of Figures

1	Comparison of DFT calculation based on "relaxed" and experimental determined crystal structure. (a) 3D Fermi surface of a theory relaxed crystal structure of BiTeI, (b) difference in "relaxed" and experimental determined crystal structures (c) 3D Fermi surface of experimental structure. DFT calculation for (d) theory "relaxed" and (e) experiment structure. Red dashed line represents experiment Fermi level. Red circles show the main difference between both DFT calculations . . . . .	8
2	Fermi surface maps of BiTeI measured at 15K using (a) 25 eV and (b) 15 eV photon energies and (c),(d) corresponding energy momentum intensity plots taken along red dashed lines in (a),(b) respectively. Red dashed lines and solid arrows are used to emphasize asymmetry in ARPES spectra. . . . .	9
3	(a) Photon energy scan at normal emission. Dashed curve represents valence band (VB) dispersion. Black solid lines represents $\Gamma$ and A points. Calculated maps (b),(d) are the FS contours implied by Fig. 1e, blurred with the Gaussian and shown in the same color scale to simulate the photoemission data. Experimental Fermi surface maps measured with (c) 22 eV ( $\Gamma$ point) and (e) 24 eV photon energies using FeSuMa electron analyzer. Photon energy range 22-24 eV is approximately 10% of $\Gamma$ - A distance in k space. . . . .	10
4	(a) Photoemission intensity plot measured at 3.2 K with 6eV laser and (b) corresponding second derivative plot . . . . .	11
5	Photoemission intensity plot obtained at 15K by using (a) 66 and (b) 74 eV photon energies. Red arrows show the position of Dirac point. (c) Constant energy ARPES momentum distribution curve ( $0.48 \pm 0.01$ eV binding energies) as a function of photon energy. . . . .	12
6	Supplementary figure. Optical conductivity, calculated for two versions of the crystal structure and for different positions of the Fermi level. . . . .	13

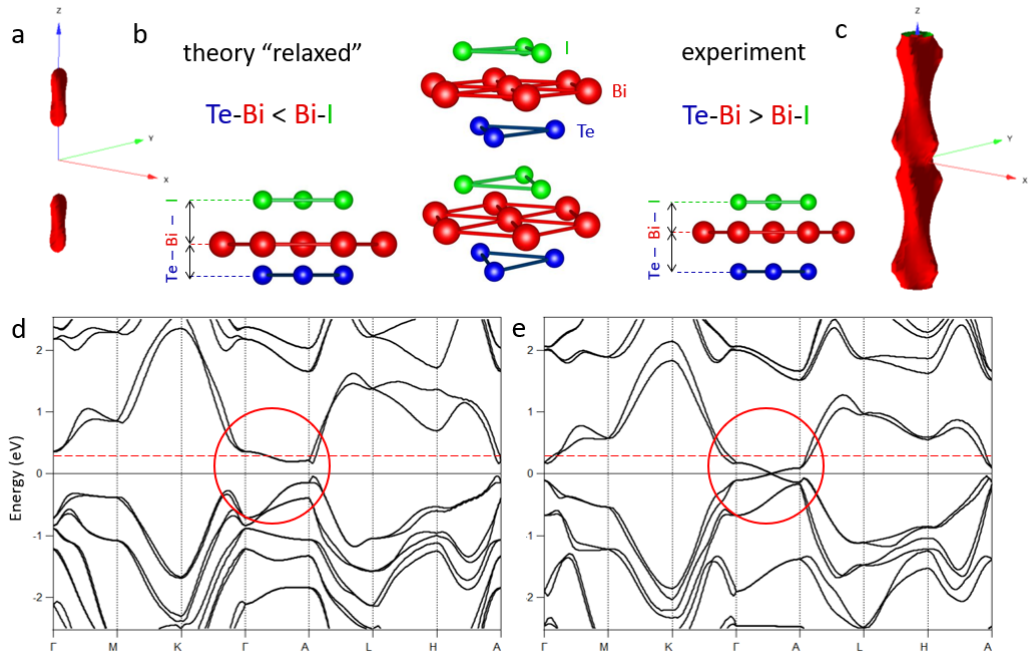


FIG. 1: Comparison of DFT calculation based on "relaxed" and experimental determined crystal structure. (a) 3D Fermi surface of a theory relaxed crystal structure of BiTeI, (b) difference in "relaxed" and experimental determined crystal structures (c) 3D Fermi surface of experimental structure. DFT calculation for (d) theory "relaxed" and (e) experiment structure. Red dashed line represents experiment Fermi level. Red circles show the main difference between both DFT calculations

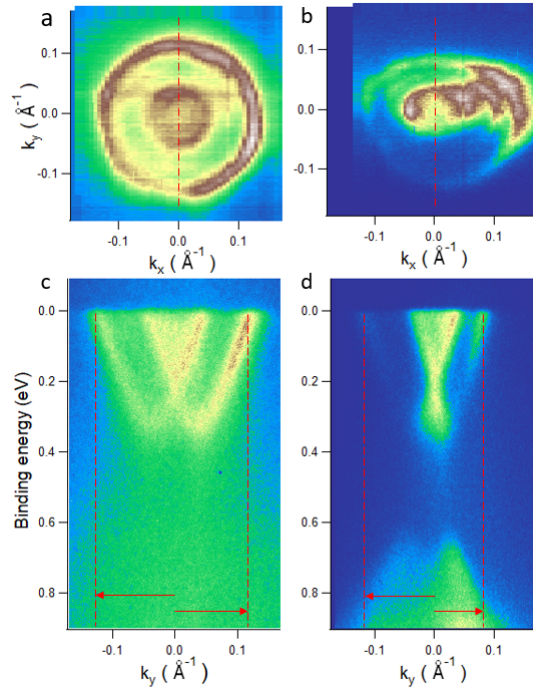


FIG. 2: Fermi surface maps of BiTeI measured at 15K using (a) 25 eV and (b) 15 eV photon energies and (c),(d) corresponding energy momentum intensity plots taken along red dashed lines in (a),(b) respectively. Red dashed lines and solid arrows are used to emphasize asymmetry in ARPES spectra.

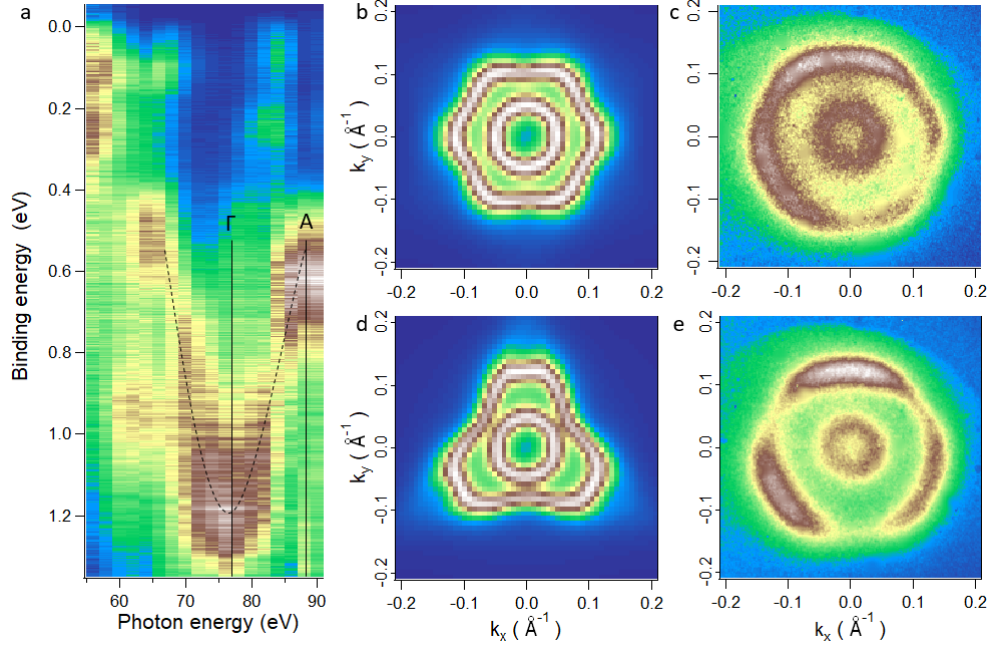


FIG. 3: (a) Photon energy scan at normal emission. Dashed curve represents valence band (VB) dispersion. Black solid lines represents  $\Gamma$  and A points. Calculated maps (b),(d) are the FS contours implied by Fig. 1e, blurred with the Gaussian and shown in the same color scale to simulate the photoemission data. Experimental Fermi surface maps measured with (c) 22 eV ( $\Gamma$  point) and (e) 24 eV photon energies using FeSuMa electron analyzer. Photon energy range 22-24 eV is approximately 10% of  $\Gamma$  - A distance in k space.

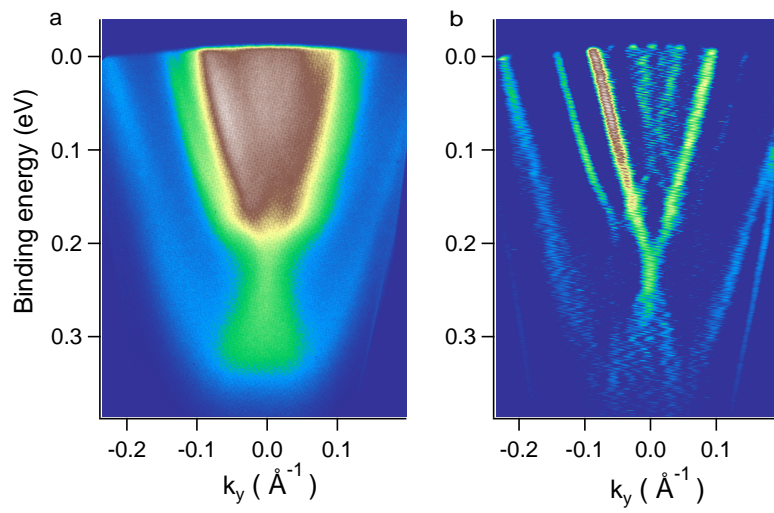


FIG. 4: (a) Photoemission intensity plot measured at 3.2 K with 6eV laser and (b) corresponding second derivative plot

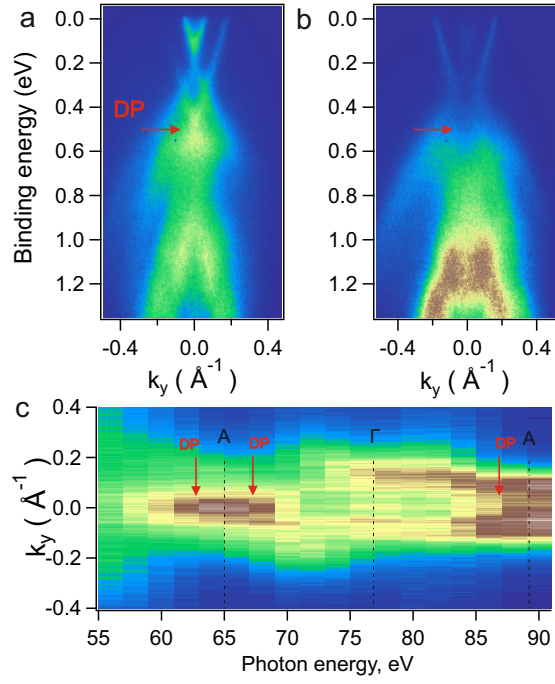


FIG. 5: Photoemission intensity plot obtained at 15K by using (a) 66 and (b) 74 eV photon energies. Red arrows show the position of Dirac point. (c) Constant energy ARPES momentum distribution curve ( $0.48 \pm 0.01$  eV binding energies) as a function of photon energy.

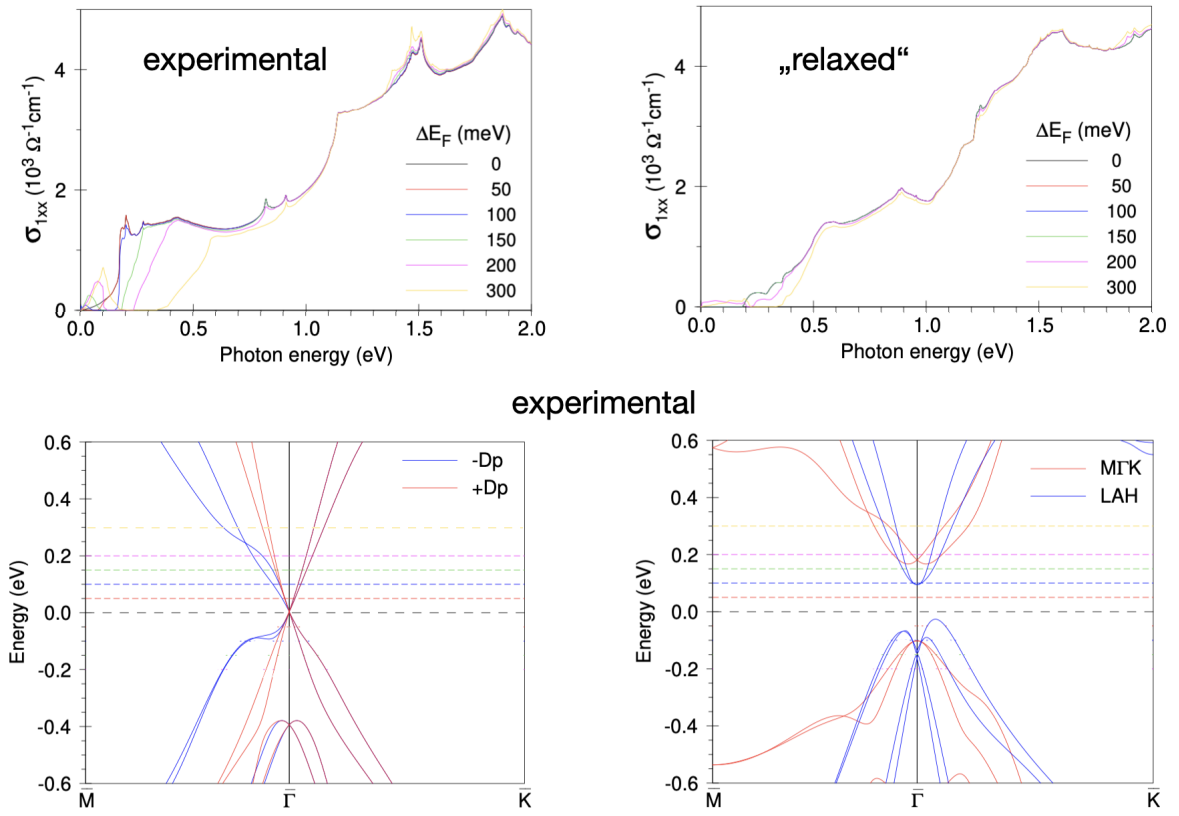


FIG. 6: Supplementary figure. Optical conductivity, calculated for two versions of the crystal structure and for different positions of the Fermi level.